PERGAMON

International Journal of Solids and Structures 38 (2001) 1669–1679

INTERNATIONAL JOURNAL OF SOLIDS and STRUCTURES

www.elsevier.com/locate/ijsolstr

Spectral element-based prediction of active power flow in Timoshenko beams

Khaled M. Ahmida *, José Roberto F. Arruda

Departamento de Mecânica Computacional, Faculdade de Engenharia Mecânica, Universidade Estadual de Campinas, C.P. 6122, 13083-970, Campinas, SP, Brazil

Received 28 July 1999; in revised form 29 March 2000

Abstract

The analysis of standing waves, which correspond to the reactive part of the power in structures, is not a sufficient tool for studying structural vibration problems. Indeed, the active power component (structural intensity) has shown to be of great importance in studying damped structural vibration problems. One of the most common numerical discretization methods used in structural mechanics is the finite element method. Although this procedure has its advantages in solving dynamic problems, it also has disadvantages mainly when dealing with high frequency problems and large complex spatial structures due to the prohibitive computational cost. On the other hand, the spectral element method has the potential to overcome this kind of problem. In this paper, the formulation of the Timoshenko beam spectral element is reviewed and applied to the prediction of the structural intensity in beams. A structure of two connected beams is used. One of the beams has a higher internal dissipation factor. This factor is used to indicate damping effect and therefore causes structural power to flow through the structure. The total power flow through a cross-section of the beam is calculated and compared to the input power. The spectral element method is shown to be more suitable to model higher frequency propagation problems when compared to the finite element method.

Keywords: Structural power flow; Structural intensity; Timoshenko beam; Spectral element method; Finite element method

1. Introduction

One of the well-known ways to efficiently analyze vibrations of frame structures with complicated boundaries and different discontinuities is the use of matrix formulations such as the finite element method (FEM). However, a large number of finite elements must be used to adequately model the distribution of the inertia of the structure. Furthermore, the higher the frequency, the larger the number of elements that must be used. The FEM can also show some computational difficulties when analyzing large frame structures, where members are usually long and too many finite elements need to be used in the discretization process. Recently, one of the potential alternative techniques being used to analyze the dynamical

* Corresponding author. Fax: +55-19-2893722.
E-mail address: khaled@fem.unicamp.br (K.M. Ahmida).

0020-7683/01/$ - see front matter
PII: S0020-7683(00)00128-1

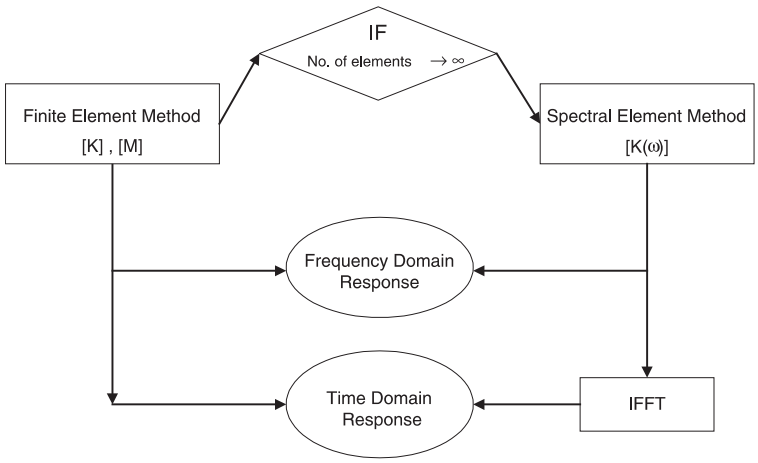

Fig. 1. Relations between FEM and SEM models.

behavior of structures is the power flow (or structural intensity) approach. The term power flow denotes the energy per unit time flowing across a surface defined within the structure by its normal. The use of power flow techniques in this kind of problem may be very useful because power flow calculation combines both force and velocity in one concept.

The measurement of structural power flow was first introduced by Noiseux (1970). In his work, bending vibrational waves obtained as a vector at a measurement point were described in terms of transverse vibrations, and then, the combined rotational and linear accelerations were used for power flow estimation considering far field conditions. The near field conditions were then included in the generalized approach. Experimental results were also used to illustrate the measurement technique. Experimental methods for measuring flexural power flow have been extensively investigated by Pavic (1976) and Verheij (1980). Power flow is usually computed experimentally from measured vibrations using finite difference approximations of the spatial derivatives that appear in the analytical formulations. The number of accelerometers used varies from two to five along each direction, depending on the assumptions made. Other methods have also been used in predicting power flow from measured vibration data: a wave component approach by Halkyard and Mace (1993), a regressive discrete fourier series (RDFS) by Arruda et al. (1996b), and a modified Prony method by Arruda et al. (1996a). Hambric and Taylor (1994) have presented a general approach that allows the application of the FEM power flow analysis to real structures by incorporating experimentally measured termination impedance as boundary conditions. This approach has been investigated on a straight beam.

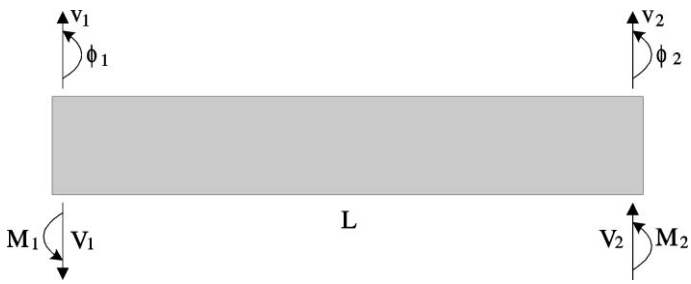

Fig. 2. Timoshenko beam with end loads and DOF.

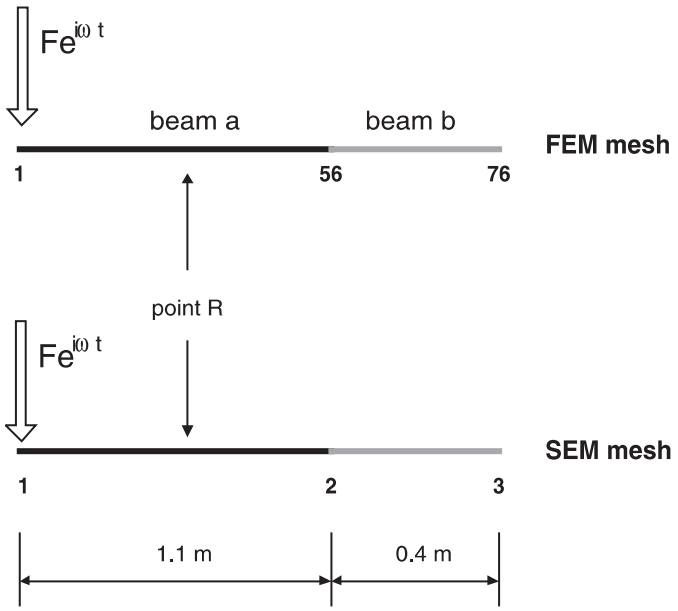

Fig. 3. FEM and SEM discretized models.

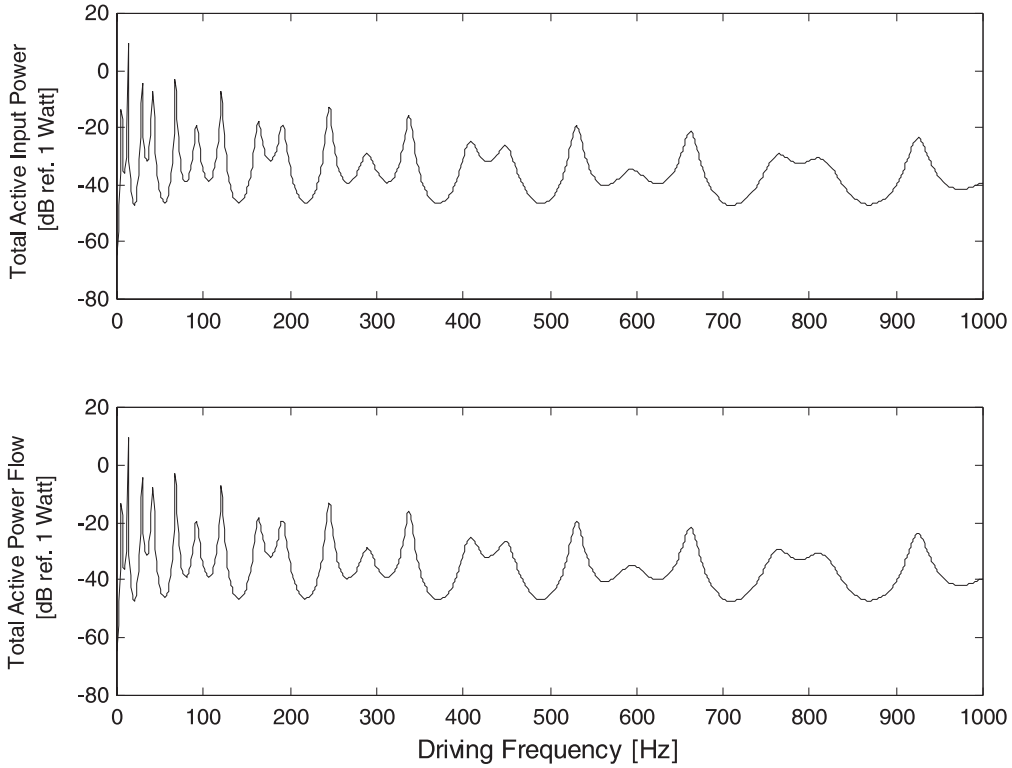

Fig. 4. Comparison of FEM predictions of input power and computed power flow at point R, at frequency range of 0–1 kHz.

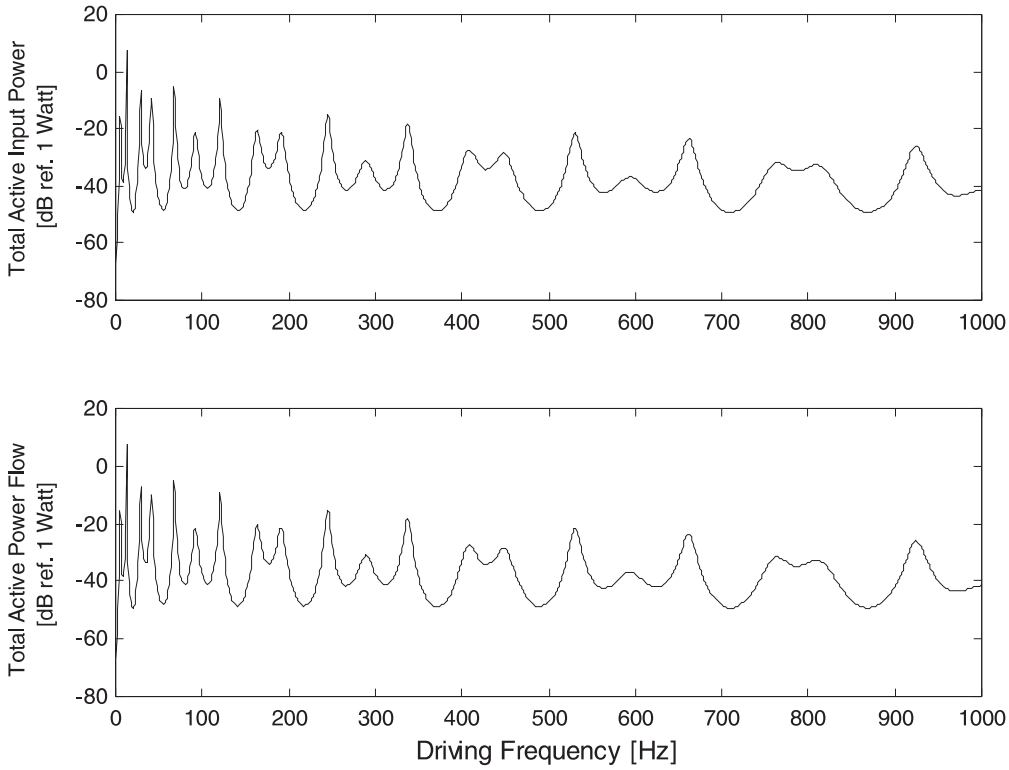

Fig. 5. Comparison of SEM predictions of input power and computed power flow at point R, at frequency range of 0–1 kHz.

In this paper, the formulations for power flow calculations are briefly reviewed. As the power flow computations are based on predicted vibration responses, these responses are obtained using FEM and the spectral element method (SEM). The SEM formulations for Timoshenko beams are described. The SEM, first presented by Doyle (1997), is formulated directly in the frequency domain and thus presents many advantages in handling vibration problems efficiently even at high frequencies. One of the advantages of this method is that it easily incorporates the use of the so-called throw-off, or semi-infinite element. This element behaves in the sense that it is a conduit for energy propagation out of the system. It can be used especially when the time of interest is short and the structure is large. This kind of element cannot be easily modeled by the conventional FEM. Therefore, the structural example used in this paper to compare FEM and SEM results does not utilize throw-off elements.

The structure used consists of two coupled straight beams. One of these beams has a higher dissipation factor. The power flow in the structure is predicted using FEM and SEM. The higher-order Timoshenko theory for beams is used in both methods.

2. Timoshenko beam spectral element

Doyle (1997) presented a spectrally formulated finite element for Timoshenko beams, known as the spectral element, to study wave propagation in beam-type structures. In contrast to the conventional finite

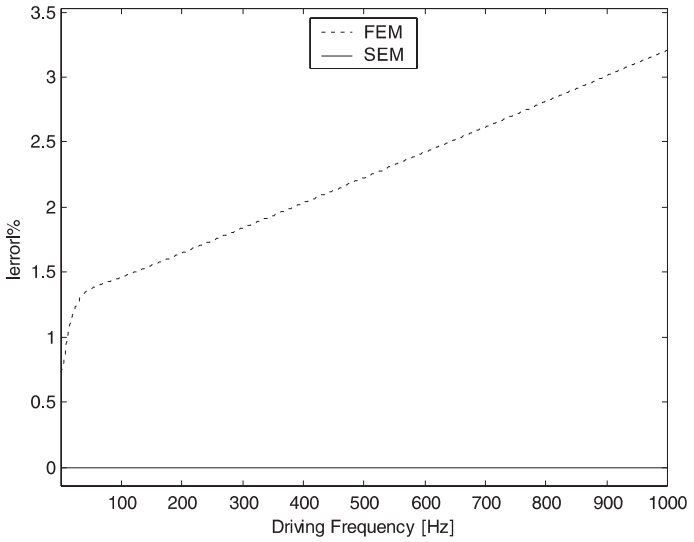

Fig. 6. Absolute error between input power and power flow computed using FEM and SEM, at frequency range of 0–1 kHz.

element, this formulation provides very accurate solutions that are based on exact shape functions and thus exact mass distribution within each structural element. This analysis, in turn, provides an accurate dynamic characterization of beam-type structures. In general, a structure is discretized into a number of spectral elements and then these elements are assembled in an analogous way to that of the FEM. The main difference is that in FEM, mass and stiffness matrices are all built and then the responses are calculated in frequency domain or in time domain. On the other hand, in SEM, the dynamic stiffness matrix is built in frequency domain and therefore, responses in frequency domain can directly be calculated. Time domain responses can then be easily obtained by performing an inverse FFT. Fig. 1 shows that SEM can be seen as a combination of the spectral methods and the assembling features of FEM. It can be shown that using one spectral element is equivalent to using an infinite number of conventional finite elements (Doyle, 1997).

For a finite Timoshenko beam, flexural waves cause two internal forces to act; bending forces and shear forces, which, in turn, cause two displacement components: transversal and rotational (Fig. 2).

Introducing shear deformation, two independent variables, $v(x,t)$ and $\phi(x,t)$, are required to describe the relevant dynamics of the beam which is governed by (Craig, 1981)

$$\begin{aligned} GA\kappa\left[\frac{\partial^2 v}{\partial x^2}-\frac{\partial \phi}{\partial x}\right] &= \rho A\frac{\partial^2 v}{\partial t^2},\\ \frac{\partial}{\partial x}EI\frac{\partial \phi}{\partial x}+GA\kappa\left[\frac{\partial v}{\partial x}-\phi\right] &= \rho I\frac{\partial^2 \phi}{\partial t^2}, \end{aligned} \tag{1}$$

where $GA\kappa$ is the shear stiffness, EI is the bending stiffness, ρA and ρI are the corresponding inertias, and κ is a geometrical constant that depends on the shape of the cross-section. The general solution of Eq. (1) can be given by the spectral representation,

$$\begin{aligned} v(x,t) &= \sum_{k=-\infty}^{+\infty}\hat{v}(x)\mathrm{e}^{\mathrm{i}\omega_k t},\\ \phi(x,t) &= \sum_{k=-\infty}^{+\infty}\hat{\phi}(x)\mathrm{e}^{\mathrm{i}\omega_k t}, \end{aligned} \tag{2}$$

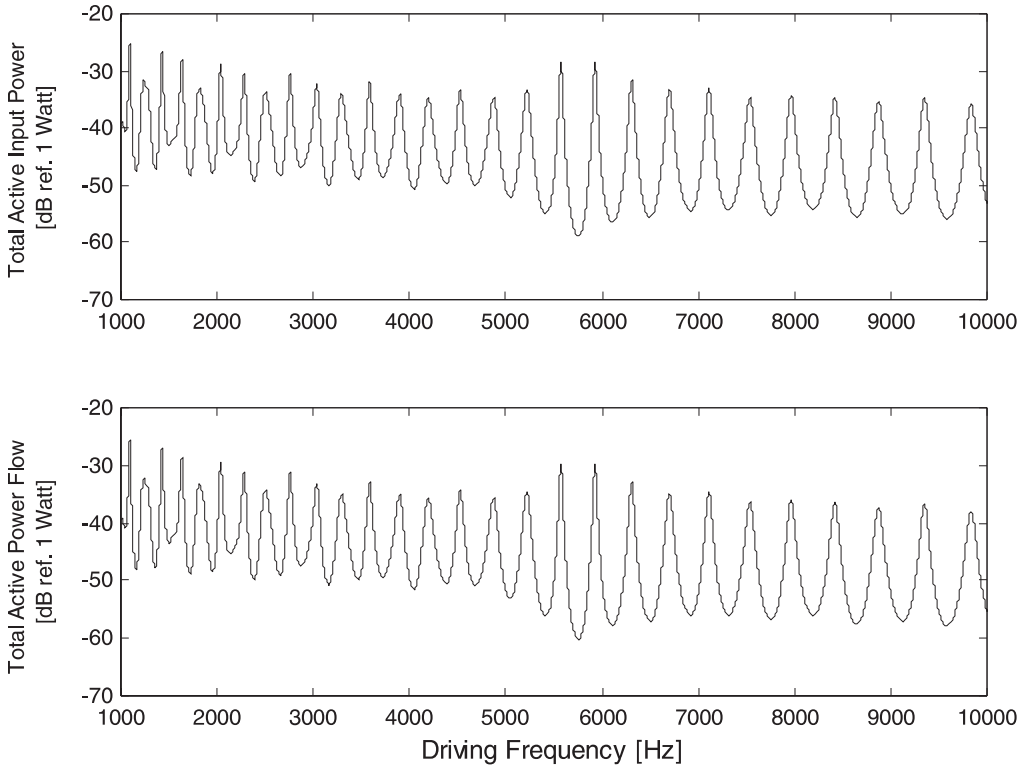

Fig. 7. Comparison of FEM predictions of input power and computed power flow at point R, at frequency range of 1–10 kHz.

where ω_k is the discrete angular frequency, $\hat{v}(x)$ and $\hat{\phi}(x)$ are spatially dependent Fourier coefficients and they are functions of ω_k, and $\mathrm{i} = \sqrt{-1}$. Assume the displacements to have a spectral representation or kernel solution functions of the form,

$$\begin{aligned} \hat{v}(x) &= P_1 \mathbf{A} \mathrm{e}^{-\mathrm{i}k_1 x} + P_2 \mathbf{B} \mathrm{e}^{-\mathrm{i}k_2 x} - P_1 \mathbf{C} \mathrm{e}^{-\mathrm{i}k_1 (L-x)} - P_2 \mathbf{D} \mathrm{e}^{-\mathrm{i}k_2 (L-x)}, \\ \hat{\phi}(x) &= \mathbf{A} \mathrm{e}^{-\mathrm{i}k_1 x} + \mathbf{B} \mathrm{e}^{-\mathrm{i}k_2 x} + \mathbf{C} \mathrm{e}^{-\mathrm{i}k_1 (L-x)} + \mathbf{D} \mathrm{e}^{-\mathrm{i}k_2 (L-x)}, \end{aligned} \tag{3}$$

where P_1 and P_2 are defined as the amplitude ratios given by

$$\begin{aligned} P_1 &= \frac{\mathrm{i}L}{GA\kappa\xi_1} \left(\frac{EI}{L^2} \xi_1^2 + GA\kappa - \rho I \omega^2 \right), \quad \xi_1 \equiv k_1 L, \\ P_2 &= \frac{\mathrm{i}L}{GA\kappa\xi_2} \left(\frac{EI}{L^2} \xi_2^2 + GA\kappa - \rho I \omega^2 \right), \quad \xi_2 \equiv k_2 L \end{aligned} \tag{4}$$

and k_1, k_2 are the wave numbers defined as

$$k_{1,2}(\omega) = \left[\frac{1}{2} \left\{ \left(\frac{1}{c_1} \right)^2 + \left(\frac{1}{c_2} \right)^2 \right\} \omega^2 \pm \sqrt{ \left(\frac{\omega}{c_2} \right)^2 + \frac{1}{4} \left\{ \left(\frac{1}{c_1} \right)^2 - \left(\frac{c_3}{c_2} \right)^2 \right\}^2 \omega^4 } \right]^{1/2}, \tag{5}$$

with the constants $c_1 \equiv \sqrt{GA\kappa/\rho A}$, $c_2 \equiv \sqrt{EI/\rho A}$, $c_3 \equiv \sqrt{\rho I/\rho A}$.

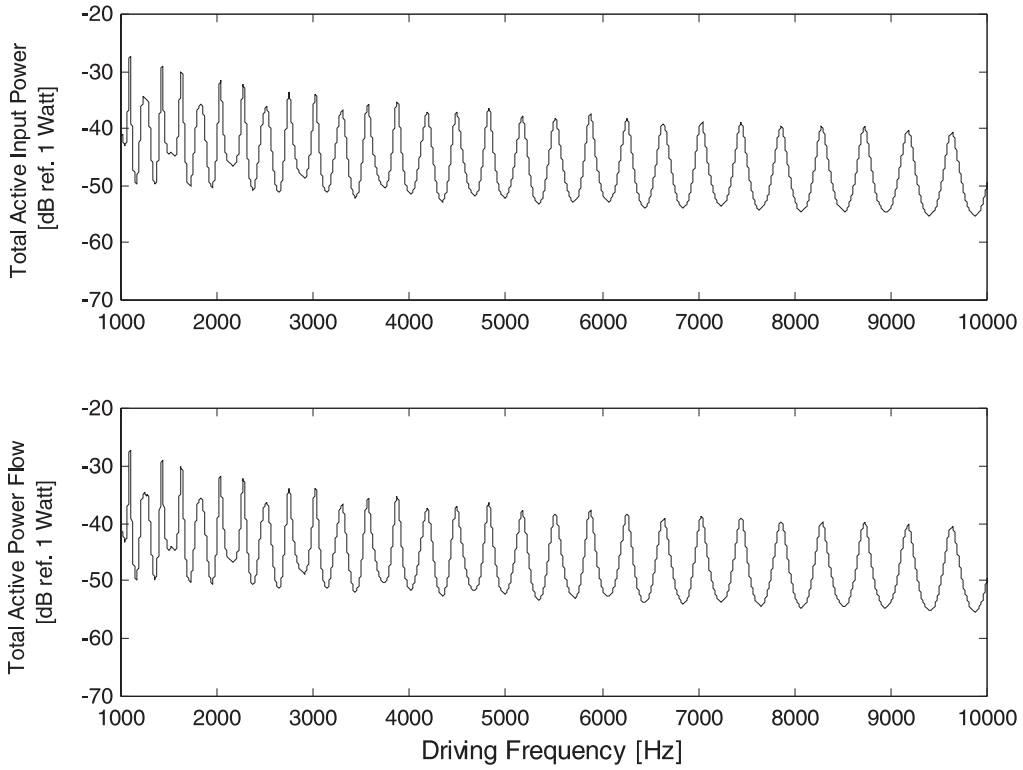

Fig. 8. Comparison of SEM predictions of input power and computed power flow at point R, at frequency range of 1–10 kHz.

For the uniform Timoshenko beam element shown in Fig. 2, the resultants of shear forces and bending moments acting on any section are related to the transversal and rotational displacements v and ϕ, respectively,

$$V(x) = GA\kappa\left[\frac{\partial v}{\partial x} - \phi\right] = -EI\frac{\partial^2\phi}{\partial x^2} + \rho I\frac{\partial^2\phi}{\partial t^2},$$
$$M(x) = EI\frac{\partial\phi}{\partial x}. \tag{6}$$

The dynamic stiffness matrix can be set up by relating the nodal displacements to the coefficients of the kernel function. The formulations that follow were found in the literature, (Doyle, 1997) but when used yielded wrong results, due to printing errors. Symbolic mathematical manipulation software (Waterloo Maple®) has been used to obtain the shape function expressions for the Timoshenko beam. By using the definitions, $\hat{v}1 = \hat{v}(0)$, $\hat{v}2 = \hat{v}(L)$, $\hat{\phi}1 = \hat{\phi}(0)$, $\hat{\phi}2 = \hat{\phi}(L)$ and $\hat{V}1 = \hat{V}(0)$, $\hat{V}2 = \hat{V}(L)$, $\hat{M}1 = \hat{M}(0)$, $\hat{M}2 = \hat{M}(L)$, the following relation can be written:

$$\begin{Bmatrix} A \\ B \\ C \\ D \end{Bmatrix} = \begin{bmatrix} P_1 & P_2 & -P_1e1 & -P_2e2 \\ 1 & 1 & e1 & e2 \\ P_1e1 & P_2e2 & -P_1 & -P_2 \\ e1 & e2 & 1 & 1 \end{bmatrix}^{-1} \begin{Bmatrix} \hat{v}1 \\ \hat{\phi}1 \\ \hat{v}2 \\ \hat{\phi}2 \end{Bmatrix} = [\hat{S}] \begin{Bmatrix} \hat{v}1 \\ \hat{\phi}1 \\ \hat{v}2 \\ \hat{\phi}2 \end{Bmatrix} \tag{7}$$

with $e1 = e^{-ik_1L}$ and $e2 = e^{-ik_2L}$.

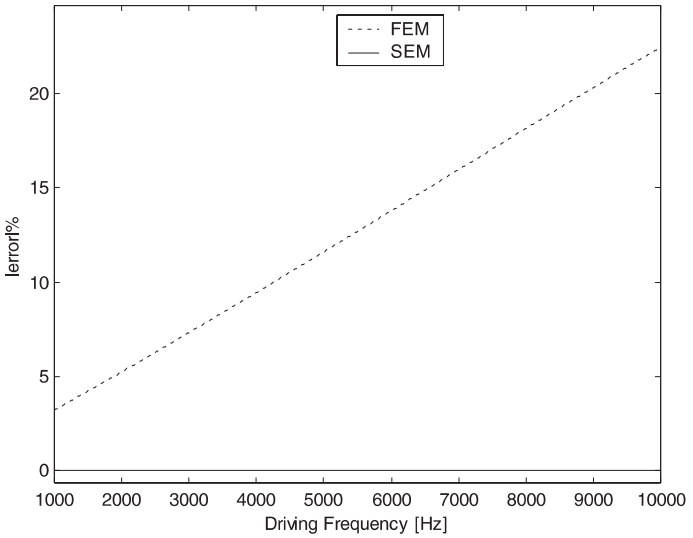

Fig. 9. Absolute error between input power and power flow computed using FEM and SEM, at frequency range of 1–10 kHz.

By using Eqs. (3) and (7), the spatial distribution of the nodal displacements can be written in the following form:

$$\begin{Bmatrix} \hat{v}(x) \\ \hat{\phi}(x) \end{Bmatrix} = \begin{bmatrix} P_1 e^{-ik_1 x} & P_2 e^{-ik_2 x} & -P_1 e^{-ik_1(L-x)} & -P_2 e^{-ik_2(L-x)} \\ e^{-ik_1 x} & e^{-ik_2 x} & e^{-ik_1(L-x)} & e^{-ik_2(L-x)} \end{bmatrix} [\hat{S}] \begin{Bmatrix} \hat{v}1 \\ \hat{\phi}1 \\ \hat{v}2 \\ \hat{\phi}2 \end{Bmatrix} = [\hat{G}] \begin{Bmatrix} \hat{v}1 \\ \hat{\phi}1 \\ \hat{v}2 \\ \hat{\phi}2 \end{Bmatrix}, \tag{8}$$

where $\lfloor \hat{G} \rfloor$ gives the shape functions for Timoshenko beam element. After the combination of Eqs. (6) and (8), the nodal forces can then be rearranged to give

$$\begin{Bmatrix} \hat{V}_1 \\ \hat{M}_1 \\ \hat{V}_2 \\ \hat{M}_2 \end{Bmatrix} = \frac{EI}{L^3} [\hat{k}] \begin{Bmatrix} \hat{v}_1 \\ \hat{\phi}_1 \\ \hat{v}_2 \\ \hat{\phi}_2 \end{Bmatrix}, \tag{9}$$

where $\lfloor \hat{k} \rfloor$ is a complex, symmetric dynamic stiffness matrix with elements given as

$$\hat{k}_{11} = (\xi_2^2 - \xi_1^2)(r_1 z_{22} + r_2 z_{21}) L/\Delta, \qquad \hat{k}_{12} = [-i\xi_2(r_1 z_{11} + r_2 z_{12}) + i\xi_1(r_1 z_{11} - r_2 z_{12})] L^2/\Delta,$$

$$\hat{k}_{13} = (\xi_1^2 - \xi_2^2)(r_1 z_{21} + r_2 z_{22}) L/\Delta, \qquad \hat{k}_{14} = [-i\xi_1(r_1 z_{12} - r_2 z_{11}) - i\xi_2(r_1 z_{12} + r_2 z_{11})] L^2/\Delta,$$

$$\hat{k}_{22} = (-i\xi_1 P_2 + i\xi_2 P_1)(r_1 z_{22} - r_2 z_{21}) L^2/\Delta, \qquad \hat{k}_{24} = (i\xi_1 P_2 - i\xi_2 P_1)(r_1 z_{21} - r_2 z_{22}) L^2/\Delta,$$

$$\hat{k}_{23} = -\hat{k}_{14}, \quad \hat{k}_{33} = \hat{k}_{11}, \quad \hat{k}_{34} = -\hat{k}_{12}, \quad \hat{k}_{44} = \hat{k}_{22}$$

with

$$r_1 = (P_1 - P_2) z_{11}, \quad r_2 = (P_1 + P_2) z_{12}, \quad \Delta = r_1^2 - r_2^2,$$

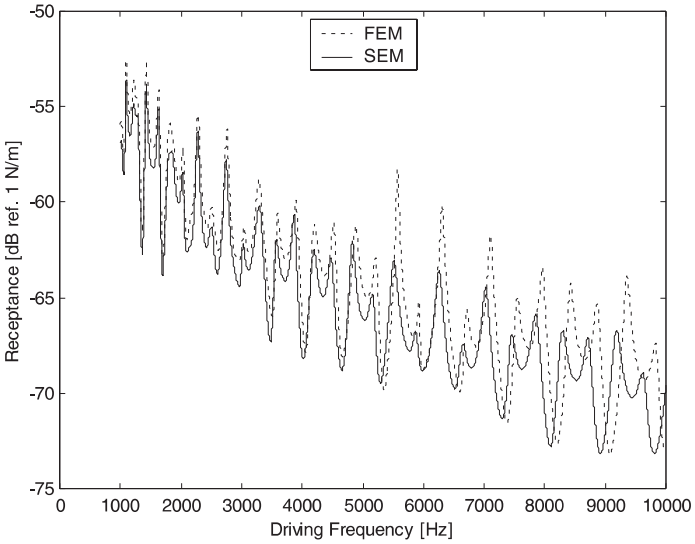

Fig. 10. Comparison of the frequency response functions at the point R obtained by the SEM- and FEM-based models, at frequency range of 1–10 kHz.

$$z_{11} = \left(1 - \mathrm{e}^{-\mathrm{i}\xi_1}\mathrm{e}^{-\mathrm{i}\xi_2}\right), \quad z_{12} = \mathrm{e}^{-\mathrm{i}\xi_1} - \mathrm{e}^{-\mathrm{i}\xi_2}, \quad z_{21} = \mathrm{e}^{-\mathrm{i}\xi_1} + \mathrm{e}^{-\mathrm{i}\xi_2}, \quad z_{22} = \left(1 + \mathrm{e}^{-\mathrm{i}\xi_1}\mathrm{e}^{-\mathrm{i}\xi_2}\right).$$

In SEM, two different types of elements can be used: 2-noded and throw-off. For throw-off element, which extends to infinity, the equations of motion can easily be established from Eq. (3) by simply putting $\mathbf{C} = \mathbf{D} = 0$, as waves propagate in only one direction. The various discretized elements in a structure can then be assembled into a global system in a way analogous to that of FEM resulting in a relation between the global shear forces and moments and the global nodal degrees of freedom written as

$$\lfloor \hat{K}_{\mathrm{g}} \rfloor \{\hat{v}_{\mathrm{g}}\} = \{\hat{F}_{\mathrm{g}}\}. \tag{10}$$

In SEM, only one element is needed between any two discontinuities, independent of its length. This plays the role of making the number of elements needed to model a structure relatively very small when compared to FEM. Therefore, the frequency response at different nodal degrees of freedom can be recovered with less computational cost, even when solving this system of equations at each frequency component. These frequency response functions can easily be used to predict the active power flow at any given point of the structure.

3. Flexural power flow in Timoshenko beams

The active power flow along a beam has two terms: the bending forces times the velocity and the bending moments times the angular velocity. For harmonic analysis, the force and the velocity are described as complex quantities and as functions of frequency. It is well established that the propagating quantity is the active component of the power, since this component is associated with energy flow. The time-averaged active power can then be defined by the real part of the power given by

$$\langle P \rangle_t = \tfrac{1}{2}\mathscr{R}\{F(\omega)\dot{v}^*(\omega)\}, \tag{11}$$

where * denotes the complex conjugate and $F(\omega)$ and $\dot{v}(\omega)$ are the complex amplitudes of the force and the velocity, respectively. The active power flow at any point along a Timoshenko beam is then given by

$$\langle P_{\mathrm{B}} \rangle_t = \frac{1}{2} \mathscr{R} \left\{ \left(-EI \frac{\partial^2 \phi}{\partial x^2} - \omega^2 \rho I \phi \right) (\mathrm{i}\omega v)^* + \left(EI \frac{\partial \phi}{\partial x} \right) (\mathrm{i}\omega \phi)^* \right\}, \tag{12}$$

where the spatial derivatives are calculated using the shape functions of the Timoshenko beam element.

4. Illustrative numerical analysis

A solution for the active power flow is sought using FEM and SEM. For this purpose, two point-coupled beams of the same cross-section (0.025 m × 0.0034 m) are used (Fig. 3). *Beam a* is an aluminum beam of length $L = 1.1$ m, with material properties given as $\rho = 2711\ \mathrm{kg\,m^{-3}}$, $E = 61 \times 10^9\ \mathrm{N\,m^{-2}}$, and null dissipation factor ($\eta = 0$) is assumed. *Beam b* is made of Lexan material of length $L = 0.4$ m, with material properties given as $\rho = 1280\ \mathrm{kg\,m^{-3}}$, $E = 2.62 \times 10^9\ \mathrm{N\,m^{-2}}$, and dissipation factor $\eta = 10\%$. This higher dissipation factor is used as an energy sink, as this energy sink is necessary to have power flow along the beam.

The structure is discretized via FEM using Timoshenko finite elements (Craig, 1981). *Beam a* is discretized into 55 finite elements, and *beam b* into 20 elements. As for SEM, only two elements are needed (Fig. 3). The excitation load is applied at the free end of *beam a*, and power flow components are calculated by FEM and SEM at a point R along *beam a*, which lies at a distance of 0.5 m from the excitation point. As the dissipation factor in *beam a* has a null value, it is eventually expected that the quantity of active power flow computed at any point along *beam a* would be exactly the same as the input power. This comparison between the input power and the active power can also be used as a validation tool for the predictions of structural power flow components.

It should be mentioned here that the throw-off element was not used here because an anechoic boundary condition completely dissipates energy out of the system, and its dynamic characteristics could not be easily modeled via FEM. It maybe interesting to notice that some localized stiffness and damping can be used at a throw-off node in order to model a boundary condition which reflects some of the incoming energy.

A frequency range of 0–1 kHz is first analyzed, which encompasses approximately the first 15 flexural modes. The FEM FRFs are computed by direct inversion of the dynamic stiffness matrix $[K - \omega^2 M]$.

Although the input power compared to the computed power flow at point R using both methods seemingly look the same (Figs. 4 and 5) due to the dB scale, there is a small difference. This percentage error is calculated at each frequency and can be seen clearly in the next figure. It can be noted that for the FEM results the error increases with the increasing frequency (Fig. 6).

Higher frequency analyses are also conducted. The error seems to increase significantly in FEM predictions. This is an expected result since the same mesh used for low frequencies has also been used for higher frequencies. On the other hand, the error in the SEM remains very small. This can be clearly established from Figs. 7–9.

It can also be noticed that resonance frequencies are different in both FEM and SEM predictions (Fig. 10). This is related to the fact that SEM predictions of frequency response are based on exact shape functions, while in FEM, predictions are based on the order of the finite element. In FEM, the error of approximation is controlled by mesh refinement (h-version) and by the polynomial's degree of elements (p-version). FEM approximations can be improved by adopting higher-order versions of FEM (p-, h- or hp-versions). However, this eventually would result in higher and undesirable computational cost.

5. Concluding remarks

There is a significant importance in studying the power flow in damped structures. These studies, when performed via the FEM, present some difficulties at higher frequencies due to high modal density and model size constraints. The SEM, on the other hand, are formulated directly in the frequency domain and thus present considerable advantages in handling such problems. This can be modeled in the FEM, but the significant difference between the input power and the computed power at a point along the beam indicates that FEM is less accurate. It should be noted that this should not occur in this case as the internal damping factor was not included in *beam a* of the model. The difference is expected to increase with frequency. In the case of the SEM, this error is significantly smaller. The SEM may fairly be well established as highly efficient method for solving high-frequency dynamic problems. In general, the spectral element method is found to provide very accurate predictions of active power flow components when compared to the conventional finite element predictions, especially at high frequencies. The disadvantage of the SEM is the small element library available. Nevertheless, SEM can be associated with FEM and BEM when complex geometries are involved (Doyle, 1997).

References

Arruda, J.R.F., Campos, J.P.R., Piva, J.I., 1996a. Experimental determination of flexural power flow in beams using a modified Prony method. Journal of Sound and Vibration 197 (3), 309–328.

Arruda, J.R.F., Campos, J.P.R., Piva, J.I., 1996b. Measuring flexural power flow in beams using a spatial-domain regressive discrete Fourier series. In: Proceedings of the 21st International Conference on Noise and Vibration Engineering. Leuven, Belgium, 641–652.

Craig, R., 1981. Structural Dynamics: An Introduction to Computer Methods. Wiley, New York, NY.

Doyle, J.F., 1997. Wave Propagation in Structures. Springer, New York, NY.

Halkyard, C.R., Mace, B.R., 1993. A wave component approach to structural intensity in beams. In: Proceedings of the 4th International Congress on Intensity Techniques. Senlis, France.

Hambric, S.A., Taylor, P.D., 1994. Comparison of experimental and finite element structure-borne flexural power measurement for a straight beam. Journal of Sound and Vibration 170 (5), 595–605.

Noiseux, D.U., 1970. Measurement of power flow in uniform beams and plates. Journal of the Acoustical Society of America 47, 238–247.

Pavic, G., 1976. Measurement of structure borne wave intensity, part I: formulation of methods. Journal of Sound and Vibration 49 (2), 221–230.

Verheij, J.W., 1980. Cross-spectral density methods for measuring structure-borne power flow on beams and pipes. Journal of Sound and Vibration 70, 133–139.